J Arid Land (2015) 7(2): 133–145
doi: 10.1007/s40333-014-0078-5
jal.xjegi.com; www.springer.com/40333

Spatial distribution of δ^2H and $\delta^{18}O$ values in the hydrologic cycle of the Nile Basin

Jeff B LANGMAN[1,2]*

[1] School of Science and Engineering, American University in Cairo, Cairo 11835, Egypt;
[2] Department of Geological Sciences, University of Idaho, Moscow 83844, USA

Abstract: Existing δ^2H and $\delta^{18}O$ values for precipitation and surface water in the Nile Basin were used to analyze precipitation inputs and the influence of evaporation on the isotopic signal of the Nile River and its tributaries. The goal of the data analysis was to better understand basin processes that influence seasonal streamflow for the source waters of the Nile River, because climate and hydrologic models have continued to produce high uncertainty in the prediction of precipitation and streamflow in the Nile Basin. An evaluation of differences in precipitation δ^2H and $\delta^{18}O$ values through linear regression and distribution analysis indicate variation by region and season in the isotopic signal of precipitation across the Nile Basin. The White Nile Basin receives precipitation with a more depleted isotopic signal compared to the Blue Nile Basin. The hot temperatures of the Sahelian spring produce a greater evaporation signal in the precipitation isotope distribution compared to precipitation in the Sahara/Mediterranean region, which can be influenced by storms moving in from the Mediterranean Sea. The larger evaporative effect is reversed for the two regions in summer because of the cooling of the Sahel from inflow of Indian Ocean monsoon moisture that predominantly influences the climate of the Blue Nile Basin. The regional precipitation isotopic signals convey to each region's streamflow, which is further modified by additional evaporation according to the local climate. Isotope ratios for White Nile streamflow are significantly altered by evaporation in the Sudd, but this isotopic signal is minimized for streamflow in the Nile River during the winter, spring and summer seasons because of the flow dominance of the Blue Nile. During fall, the contribution from the White Nile may exceed that of the Blue Nile, and the heavier isotopic signal of the White Nile becomes apparent. The variation in climatic conditions of the Nile River Basin provides a means of identifying mechanistic processes through changes in isotope ratios of hydrogen and oxygen, which have utility for separating precipitation origin and the effect of evaporation during seasonal periods. The existing isotope record for precipitation and streamflow in the Nile Basin can be used to evaluate predicted streamflow in the Nile River from a changing climate that is expected to induce further changes in precipitation patterns across the Nile Basin.

Keywords: Nile River; arid environment; deuterium excess; regional climate model uncertainty; evaporation isotope effects

Citation: Jeff B LANGMAN. 2015. Spatial distribution of δ^2H and $\delta^{18}O$ values in the hydrologic cycle of the Nile Basin. Journal of Arid Land, 7(2): 133─145. doi: 10.1007/s40333-014-0078-5

The stable isotopes of water (represented as δ^2H or $\delta^{18}O$) are useful environmental tracers because of isotope fractionation during water phase changes (Gonfiantini et al., 1998), which produces an isotopic signal associated with temperature-induced processes such as evaporation (Gat, 2001). Understanding regional or basin dynamics of these processes is important for developing useful water budgets and predicting resource availability (Risi et al., 2010). Differences in air temperature and relative humidity will substantially influence isotopic fractionation (Gat, 1996), and regional land characteristics can influence the fractionation process (Poage and Chamberlain, 2001; Liotta et al., 2006). Additionally, the differences in diffusivity of hydrogen and oxygen isotopes will produce a secondary isotopic signal (deuterium excess

*Corresponding author: Jeff B LANGMAN (E-mail: jlangman@uidaho.edu)
Received 2013-11-22; revised 2014-02-17; accepted 2014-07-26

or d-excess), which allows for further discrimination of basin processes that influence water resources (Risi et al., 2010). The increased understanding of isotopic fraction in the hydrologic cycle has allowed the incorporation of the water isotopes in regional climate models, although their utility is derived from the extent of isotopic data coverage and the understanding of basin processes that influence fractionation processes (Hoffmann et al., 2000; Mathieu et al., 2002; Noone and Simmonds, 2002; Sturm et al., 2005).

Regional climate or hydrologic models have been used to estimate Nile River streamflow (Gleick, 1991; Hulme, 1994; Conway et al., 1996; Conway and Hulme, 1996; Yates and Strzepek, 1998; Strzepek et al., 2001; Eldaw et al., 2003; Buontempo et al., 2009; Elshamy et al., 2009; Booij et al., 2011), even though the outputted precipitation and subsequent streamflow predictions have large temporal and spatial uncertainty (Hulme et al., 2001; Buontempo et al., 2009). The multi-model approach compiled by the Intergovernmental Panel on Climate Change indicates rising temperatures throughout the Nile Basin and substantial uncertainty in future precipitation patterns (Conway, 2005; Beyene et al., 2010). Quantifying inter-annual rainfall variability, particularly in the Sahel, is systematically difficult and likely unreliable given current climate model forcing (low convergence for rainfall predictions) (Hulme et al., 2001; Conway, 2005; Elshamy et al., 2009; Risi et al., 2010). This study reviewed existing Nile Basin precipitation and surface-water isotopic composition to better understand the basin processes that influence precipitation and streamflow, which may assist in reducing the uncertainty of predicted precipitation and streamflow in the Nile River and its tributaries.

1 Study area

The Nile River is fed by two main tributaries—the White Nile with its watershed in the equatorial Lake Plateau Region (Burundi, Rwanda, Tanzania, Kenya, Zaire and Uganda), and the Blue Nile with its watershed in the Ethiopian Highlands (Fig. 1). The White Nile and Blue Nile converge near Khartoum, Sudan, and the resulting Nile River flows through the eastern Sahel and eastern Sahara in northern Sudan and Egypt where water demand is the highest because of the arid climate. High evaporation in the Lake Plateau Region reduces the contribution of the White Nile, and 70% of the annual streamflow and upwards of 80% of the high-flow season streamflow of the Nile River is attributed to flow from the Blue Nile and a small contribution from the Atbara River (Johnson and Curtis, 1994; Booij et al., 2011). With the dominance of the Blue Nile on overall Nile River streamflow (Fig. 2), the Nile River exhibits a unimodal distribution with an increase in flow beginning in June and ending in November and relatively low flow from December through May for the southern Nile Basin (Booij et al., 2011). Flow in the Nile River downstream of Lake Nasser in Egypt (northern Nile Basin) is heavily regulated, and the release from Aswan High Dam is dependent upon irrigation needs of downstream users such as larger releases during summer months (Abu-Zeid and El-Shibini, 1997). The Nile River has historically seen large multi-year precipitation and hydrologic fluctuations (Conway and Hulme, 1996; Conway, 2005), and hydrologic sensitivity analyses indicate that small changes in precipitation in the upper watershed could substantially impact water availability (Conway and Hulme, 1996; Yates and Strzepek, 1998; Conway, 2005; Beyene et al., 2010).

Climate in the Nile Basin includes humid equatorial, seasonally-arid tropical, semi-arid, and arid inland types and a sub-tropical coastal types. There is a sharp precipitation gradient with the transition from the humid equatorial region to the semi-arid Sahel (generally located between 15º–20ºN latitude across Africa (Nicholson, 1994)) and the arid Sahara. Two distinct marine sources of water vapor are present for the Nile Basin—the Mediterranean and western Indian Ocean. Moisture moves in from the Mediterranean or across North Africa during the winter months and can influence the northern Nile Basin, and moisture is driven into the southern Nile Basin during the Indian Ocean monsoon season in summer months (El-Asrag, 2005). The wet period of the Ethiopian Highlands (Blue Nile region) occurs from July through September and is the main driver of Nile River streamflow (Johnson and Curtis, 1994; Yates and Strzepek, 1998). Climate in the White Nile Basin (Lake Plateau Region) is driven by African equatorial circulations and is not correlated with the marine moisture of the Indian

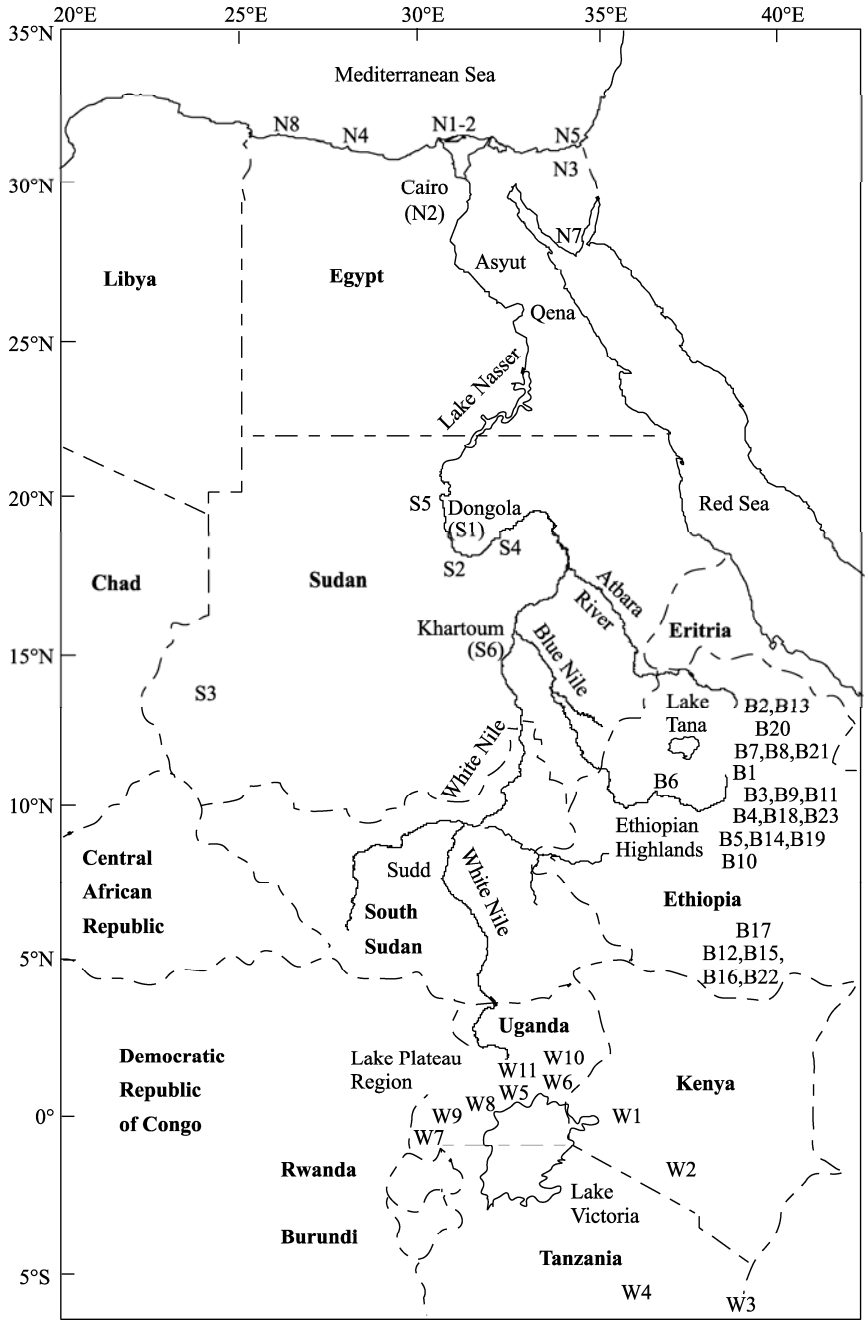

Fig. 1 Nile River and its tributaries—White Nile, Blue Nile and Atbara River with precipitation collection sites indicated. N, northern Nile Basin; S, southern Nile Basin; B, Blue Nile Basin; W, White Nile Basin.

Ocean (Sestini, 1993). Substantial rainfall occurs in the Lake Plateau Region, but much of it is lost to evapotranspiration, which minimizes the contribution of the White Nile to the overall Nile River streamflow (Booij et al., 2011).

The Ethiopian Highlands are where the Sahelian moisture flux (South Atlantic moisture source) and the Indian Ocean circulations merge (Awadallah and Rousselle, 2000). The wet season in the Ethiopian Highlands is a result of the northward movement of the intertropical convergence zone (ITZC) from West Africa across the continent and tropical moisture drawn in from the Indian Ocean to the southern Nile Basin (Camberlin, 1997). The dry season is a result of the influx of drier air masses from the north out of the Sahara or Arabian Peninsula (Seleshi and Zanke,

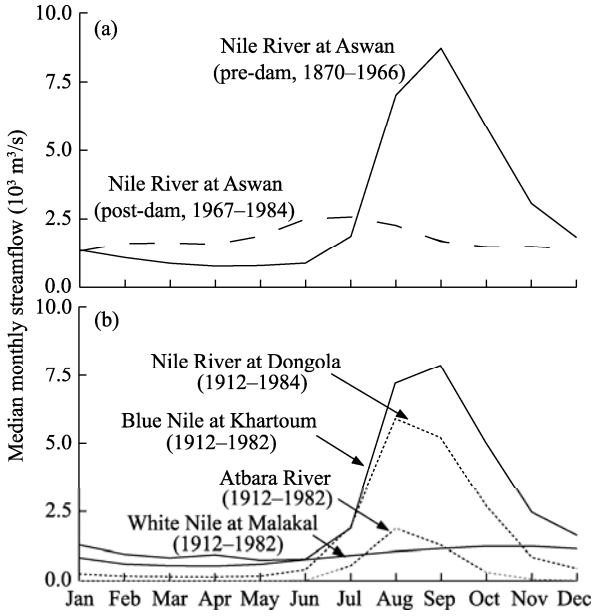

Fig. 2 Nile River and tributary streamflow

2004). Eltahir (1996) and Amarasekera et al. (1997) suggested that 20%–25% of the natural variability of flow in the Nile can be attributed to El Nino–Southern (ENSO) oscillations. Studies also have tried to correlate Nile flows to climate patterns such as Quinn's (1992) and Whetton and Rutherfurd's (1994) use of historical Nile streamflow to evaluate the intensity of the ENSO phenomenon. Decadal and multi-decadal variability is common in the Nile Basin, particularly in the Sahel (Sun et al., 1999; Hulme et al., 2001), and oscillation of the ITZC correlates with ENSO (Sun et al., 1999; Hulme et al., 2001; Seleshi and Zanke, 2004).

The eastern Mediterranean typically has higher d-excess precipitation compared to the western Mediterranean (median of 14‰ and 22‰, respectively), because of the trajectory of air masses (IAEA, 2005) and large humidity deficits (Gat et al., 2003). Precipitation d-excess typically increases moving southeastward across the Mediterranean with values greater than 18‰ along the Egyptian coast from Alexandria eastwards through Sinai (Gat and Carmi, 1970). D-excess values increase in winter months for the northern Nile Basin because of greater atmospheric stability (larger surface pressure and less wind persistence), and the d-excess decreases southward in the basin (El-Asrag, 2005). Precipitation in the eastern Mediterranean is typically enriched with ^{2}H and ^{18}O during the dry season (late spring and summer), but the lack of rainfall during this period reduces the influence of this precipitation on surface water (Gat and Dansgaard, 1972). Similar analyses have not been conducted for the White Nile Basin and Blue Nile Basin at a regional scale (IAEA, 2005).

2 Methods

Water-isotope data were compiled from the International Atomic Energy Agency (IAEA) Water Resources Programme's Isotope Hydrology Information System database, which contains precipitation isotope data (Global Network of Isotopes in Precipitation (GNIP)) and surface-water isotope data (Global Network of Isotopes in Rivers (GNIR)) from numerous projects conducted within the Nile Basin (Fig. 1; Tables 1–2; Appendix 1). Precipitation samples were collected in cooperation with the World Meteorological Organization (WMO), national meteorological services, national authorities and various academic partners (IAEA, 2014). Precipitation samples were collected only from official WMO stations and the samples primarily were analyzed by the IAEA's Isotope Hydrology Laboratory in Vienna (Appendix 1), although some samples were measured in cooperating laboratories (IAEA, 2014). Sample collection, sample submission and sample analysis were reviewed by the IAEA's Water Resource Programme prior to inclusion in the GNIP and GNIR databases. The data were divided by region (White Nile, Blue Nile, Sahel and Mediterranean (Sahel to Mediterranean Sea)) and by northern hemisphere season designation—fall (September through November), winter (December through February), spring (March through May) and summer (June through August). The Nile Basin receives precipitation from two main water vapor sources—Mediterranean Sea (including some contribution from the Atlantic Ocean) and the Indian Ocean. These distinct sources provide the majority of water vapor during particular seasonal periods—winter for the Mediterranean Sea and late spring, summer (monsoon) and early fall for the Indian Ocean, and in different temperature/climate regimes between the arid northern part and tropical southern part of the basin. The distribution of $\delta^{2}H$,

$\delta^{18}O$ and d-excess were examined according to these regional and seasonal partitions to better understand the isotopic signal of precipitation in the streamflow generating regions (White Nile and Blue Nile) and the influence of evaporation and limited rainfall north of the confluence of the White Nile and Blue Nile (Sahel, Sahara and near the Mediterranean coast).

Table 1 Collection site information and number of samples collected for isotope analysis of precipitation in the Nile Basin

Watershed	Region and collection site	Data record	Total $\delta^{18}O$	Total δ^2H
White Nile	Equatorial Lake Plateau Region	1960–2009	479	462
	Kenya: Kericho (W1), Mugaga (W2) Tanzania: Dar es Salaam (W3), Dodoma (W4) Uganda: Entebbe (W5), Jinja (W6), Kisoro (W7), Masaka (W8), Rukungiri (W9), Soroti (W10), Wobulenzi (W11)			
Blue Nile	Ethiopian Highlands (Ethiopia)	1961–2009	474	470
	Addis Ababa (B1), Adu Bariye (B2), Alemeya (B3), Asela (B4), Awassa (B5), Butajira (B6), Combolcha (B7), Dessie (B8), Diredawa (B9), Hagere Selam (B10), Harar (B11), Hidolola (B12), Kobo (B13), Kofele (B14), Mega (B15), Moyale (B16), Neghelle (B17), Silte (B18), Soddo (B19), Weldiya (B20), Weledi (B21), Yavello (B22), Ziway (B23)			
Nile River, Sahel	Central Sudan	1962–1997	92	77
	Dongola (S1), Al Dabbah (S2), Geneina (S3), Karima (S4), Kerma (S5), Khartoum (S6)			
Nile River, Sahara	Northern Egypt/Mediterranean	1961–2004	266	258
	Alexandria (N1), Cairo (N2), El-Arish (N3), Marsa Matruh (N4), Rafah (N5), Ras Eltine (N6), Saint Catherene (N7), Siddi Barrani (N8)			

Note: The data source is the isotope record compiled by the International Atomic Energy Administration's Water Resources Programme and archived in the Global Network of Isotopes in Precipitation database. The numbers in the last two columns indicate the number of samples for each isotope analysis.

Table 2 Collection site information and number of samples collected for isotope analysis of surface water samples in the Nile Basin

Watershed	Region and surface water types	Data record	Total $\delta^{18}O$	Total δ^2H
White Nile	Lake Victoria (1,130 to 1,250 m asl)	1988–2006	262	263
	Various locations along the lake shoreline in Kenya, Tanzania, and Uganda			
	Rivers (400 to 1,210 m asl)	1970–2005	66	65
	Various rivers in the Lake Plateau region including the White Nile and tributaries to Lake Victoria and the White Nile			
Blue Nile	Downstream of the Ethiopian Highlands (385 to 500 m asl)	1970–1997	25	25
	Various locations along the Blue Nile in Sudan			
Nile River, Sahel	Central Sudan (350 to 390 m asl)	1970–1993	16	16
	Various locations downstream of Khartoum on the mainstream of the Nile River			
Nile River, Sahara	Northern Egypt/Mediterranean (100 to 310 m asl)	1981–1995	28	8
	Various locations on the mainstream and canals of the Nile River between Qena and Asyut, Egypt			

Note: The data source is the isotope record compiled by the International Atomic Energy Administration's Water Resources Programme and archived in the Global Network of Isotopes in Rivers database. The numbers in the last two columns indicate the number of samples for each isotope analysis.

Isotopic trendlines were determined by least squares regression (a comparison of least squares and robust regressions indicated that least squares regression provided a more accurate trendline fit). The coefficient of determination (R^2) is presented to indicate the goodness of fit of the least squares regression. The process of water vapor formation and precipitation can be viewed through the alteration of the water isotope ratios and, in particular, the alteration of trendline characteristics (slope and intercept (d-excess)), which can be good indicators of the source of precipitation (Dansgaard, 1964; Craig and Gordon, 1965). D-excess in atmospheric moisture is a result of evaporation at the air-water interface and different isotopologues of water ($^1H_2{}^{16}O$, $^1H^2H^{16}O$, $^1H_2{}^{18}O$, $^1H_2{}^{17}O$) that have different saturation vapor pressures and different diffusion rates, which provide further fractionation in this boundary layer (Dansgaard,

1964; Craig and Gordon, 1965; Merlivat and Jouzel, 1979). The level of d-excess is primarily influenced by water vapor sources (Dansgaard, 1964; Craig and Gordon, 1965; Merlivat and Jouzel, 1979) and acts as an additional isotopic signal for discriminating precipitation sources.

To evaluate the influence of the contributing regions to the Nile River and the influence of evaporation on the isotopic signal of the river, precipitation isotopic characteristics were compared to the Global Meteoric Water Line (GMWL; Craig, 1961):

$$\delta^2H=8.13\delta^{18}O+10.8‰. \quad (1)$$

Changes in the slope of the δ^2H-$\delta^{18}O$ relation are indicative of evaporation. Lower slopes suggest greater evaporation, and distributions spreading along the trendline can indicate differences in temperatures during precipitation formation—colder for more depleted values and warmer for more enriched values (Rozanski et al., 1993). Additionally, precipitation vapor sources can be discerned with more arid (possibly continental) sources that can be shifted above the GMWL and more humid vapor sources shifted below the GMWL. A comparison of isotope signals between waterbodies (e.g. river and precipitation) can be viewed through the change in fractionation factor (α):

$$\alpha=({}^{h}a/{}^{l}a)/({}^{h}b/{}^{l}b)=R_a/R_b. \quad (2)$$

Where the ratio (R) of the heavy (h) and light (l) isotopes of two sources (a and b) is altered with changes in the sources.

3 Results and discussion

Isotopic variation in the Nile River should be driven by seasonal climate changes in the Blue Nile Basin, followed by a lesser influence from seasonal influences in the White Nile Basin (Sestini, 1993; Camberlin, 1997; Awadallah and Rousselle, 2000; Booij et al., 2011). Additionally, the increasing evaporation effect with northward flow through the semi-arid and arid areas should alter the surface-water isotope signal, and a final influence may be seen in northern Egypt with a limited Mediterranean-driven precipitation input. The following analysis examines these influences and the alteration of the isotopic signal with northward flow of the Nile River from its headwaters in the Equatorial Lake Plateau Region (White Nile) and the Ethiopian Highlands (Blue Nile).

There is substantial regional and seasonal variation in the isotopic signal of precipitation throughout the Nile Basin (Fig. 3), but each seasonal period in each region has an identifiable isotopic signal with variable slope and intercept values (R^2 values≥0.83 except for the fall season in the Mediterranean region (R^2=0.66)). The White Nile Basin (slope: 6.6–7.6) receives precipitation more similar to the GMWL slope compared to the Blue Nile Basin (slope: 6.3–7.1) except during the summer and fall seasons (slopes: 7.0 and 7.1, respectively) when rainfall in the Blue Nile Basin is driven by the Indian Ocean monsoon. The precipitation isotopic signal of the White Nile is a result of a more continental source of precipitation (arid vapor source) compared to the Indian Ocean source of the Blue Nile. This inland precipitation generates an isotopic distribution that has a greater central tendency and range of depleted values (Fig. 3), which likely is a result of greater temperature and altitude differences associated with continental vapor sources (Rozanski et al., 1993; Gat, 2001). Trendline slopes for the Sahel (slope: 6.0–6.6) and Mediterranean (slope: 5.4–6.3) regions indicate lower values because of greater evaporation compared to the White Nile and Blue Nile precipitation (Fig. 3). The Mediterranean region receives the most depleted precipitation across all available seasons (no summer data), which is consistent with the isotopic signal of the eastern Mediterranean precipitation as described by Gat and Dansgaard (1972) and El-Asrag (2005). The Sahel and Blue Nile regions share similar isotopic signals during available seasons (insufficient winter data for the Sahel). The similarity of isotopic signals for Sahel and Blue Nile precipitation is a result of the inward flow of summer monsoon moisture from the Indian Ocean that provides moisture to these two regions (El-Asrag, 2005), unlike the White Nile moisture that is driven by continental convective currents (Sestini, 1993). A statistical comparison (Wilcoxon rank-sum test) of seasonal precipitation data for the Sahel and Blue Nile regions indicates similar distributions for spring $\delta^{18}O$ (P=0.02) and δ^2H (P=0.1) and mixed similarity/dissimilarity during summer (P=0.4 for $\delta^{18}O$ and P=0.01 for δ^2H) and fall (P=0.08 for $\delta^{18}O$ and P=0.6 for δ^2H).

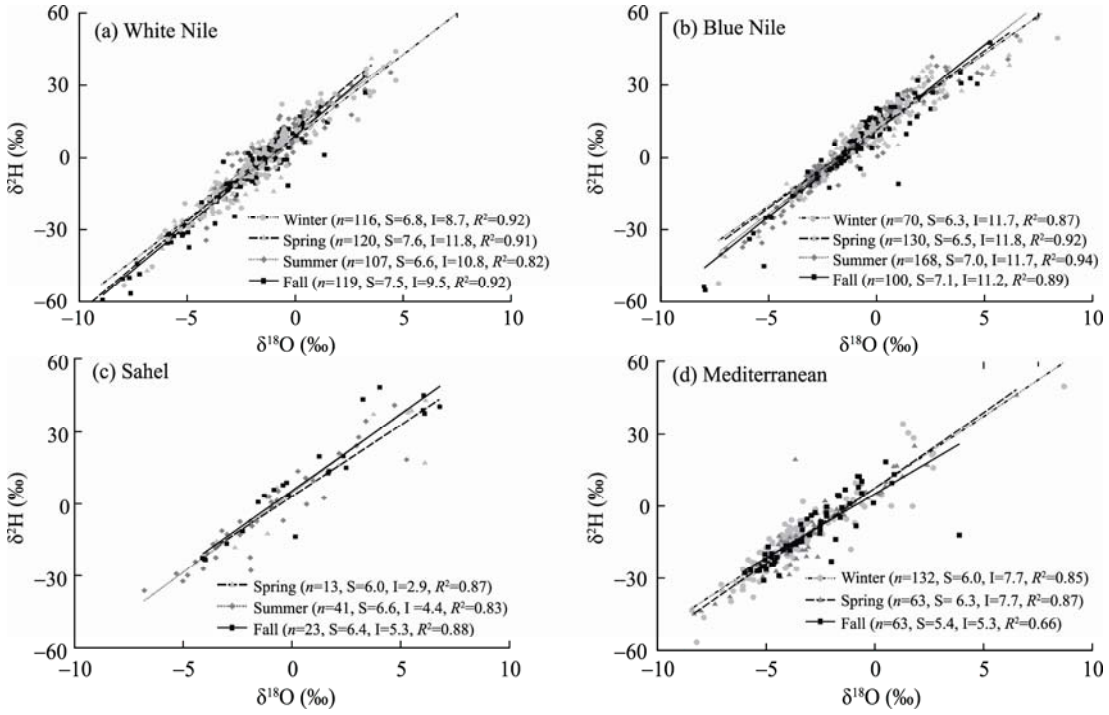

Fig. 3 Seasonal variation in the isotopic composition of precipitation in the four regions of the Nile Basin (least squares linear regression trendlines with number of data points (*n*), slope (S), intercept (I) and coefficient of determination (R^2))

Variation of the isotopic composition of precipitation is more easily viewed through a seasonal comparison of trendline characteristics of each region (Fig. 4). The trendlines reflect differences in source waters, evaporation/condensation (temperature effect), and inter-isotope fractionation (d-excess generation). A larger evaporation effect is apparent for the Sahel and Mediterranean regions as indicated by lower slopes and smaller d-excess (intercept) of these regions compared to the White Nile and Blue Nile regions (Fig. 4), which is consistent with climate differences between the southern and northern regions. The source waters of the Nile River that originate in the White and Blue Nile regions have similar isotopic trend characteristics throughout each season (Fig. 4) but differ in their distribution characteristics (Fig. 3). The fall trendlines present an expected rotation towards a more evaporated signal with northward movement from the headwaters into the drier Sahel and Sahara. The spring trendlines do not conform to this expected evaporation effect as the Sahel presents a precipitation isotopic signal of greater evaporation than the Sahara dominated Mediterranean region. This difference can be explained by the annual temperature variation of the Sahel where spring is generally the hottest season because summer is cooled by the influx of water vapor from the Indian Ocean monsoon flow (Guichard et al., 2009), which does not occur in the eastern Sahara.

The isotopic signal of precipitation in the source-water regions is conveyed to local streamflow and further altered with additional evaporation according to the local climate. All surface waters indicate identifiable seasonal signals (R^2 values≥0.71) with variable slope and intercept values except for the spring season at Lake Victoria (R^2=0.1), which has two distinct data groups that do not conform to a linear trend. The seasonal isotopic signal of Lake Victoria indicates an evaporated signal during all seasons compared to White Nile precipitation (trendline characteristics of Figs. 3 and 5). The isotopic signal of Lake Victoria is further altered by additional evaporation with flow through the White Nile (generally lower trendline slopes of the White Nile compared to Lake Victoria), although this additional evaporated signal is relatively small. It is expected that the White Nile has an even greater evaporated signal prior to its confluence with the Blue Nile because of evaporation with flow through the

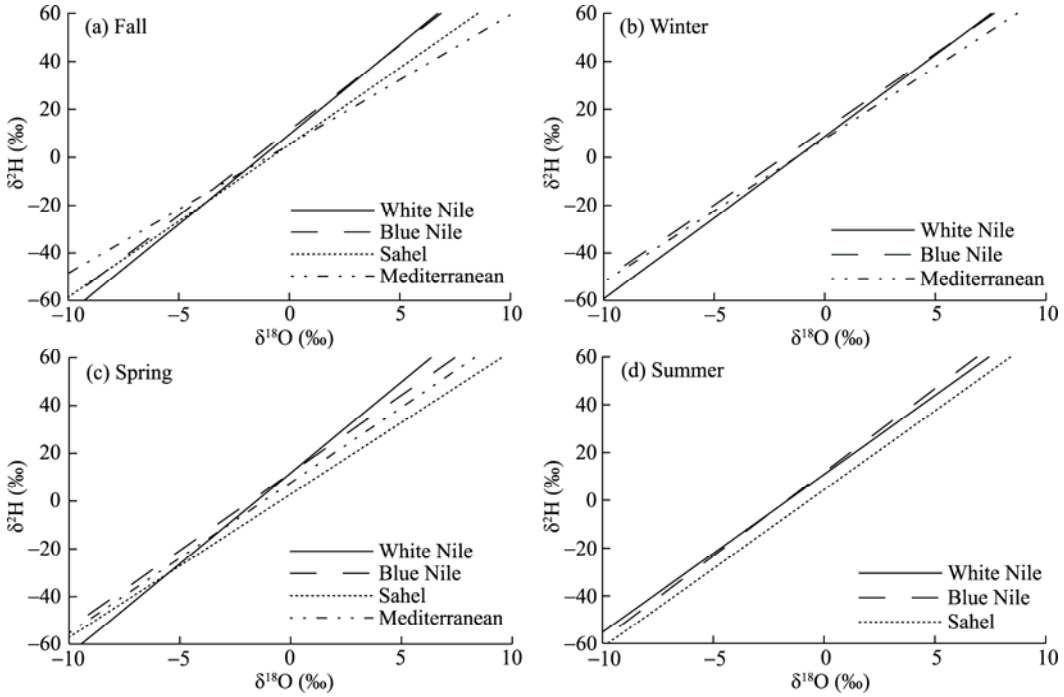

Fig. 4 Least squares linear regression trendlines for seasonal isotopic composition of precipitation across the four regions (White Nile, Blue Nile, Sahel and Mediterranean) of the Nile Basin

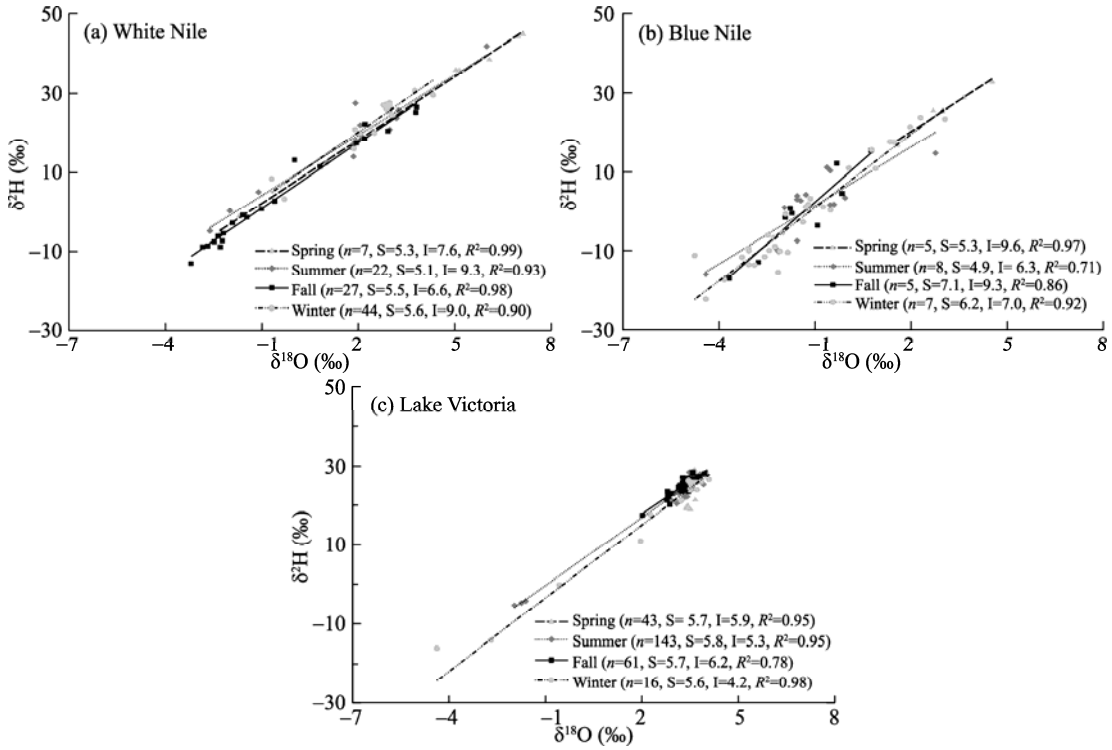

Fig. 5 Seasonal variation in the isotopic composition of streamflow in the White Nile and Blue Nile (least squares linear regression trendlines with number of data points (n), calculated slope (S), intercept (I) and coefficient of determination (R^2))

Sudd (or Bahr al Jabal, a vast 500 km×200 km swamp), and this evaporative signal is visible in the distribution of isotopic data for the White Nile streamflow. Isotopic data upstream of the Sudd had an overall median $\delta^{18}O$

of –2.05‰ and δ^2H of –4.8‰, and the median values downstream of the Sudd were 2.43‰ for $\delta^{18}O$ and 21.8‰ for δ^2H, indicating a very strong evaporation effect on White Nile streamflow through the Sudd. The White Nile region loses substantial surface water to evaporation (Booij et al., 2011), which drastically changes the isotopic signal of the White Nile streamflow. The heavy isotopic signal of the White Nile is masked by the lighter signal of the Blue Nile that dominates the isotopic signal of the combined streamflow of the Nile River downstream of Khartoum.

The isotopic relation of precipitation to streamflow and upstream to downstream streamflow can be viewed through changes in fractionation factors (α), which represents the amount of fractionation during an exchange reaction (e.g. condensation or evaporation). The fractionation factor of resulting river water compared to its regional precipitation indicates that the heavier isotopes are concentrated in the subsequent river samples (α>1 indicates heavy isotope concentration in the numerator or the product of the exchange reaction such as the river in this example) except for the Blue Nile, which only indicates this relation during spring (Table 3). The concentration of heavier isotopes in the river is expected with evaporation, but the lack of concentration of heavier isotopes in surface water in the Blue Nile region may be because of the influence of the Indian Ocean monsoon that would reduce evaporation. The lower value fractionation factors for comparing White Nile to Sahel Nile River flow exemplifies the lack of influence of the White Nile on the Nile River (Table 4). Except for fall, the fractionation factor is less than one for all seasons between the White Nile and Sahel because of high evaporation in the Sudd, and this heavy signal is subsequently diluted in the Nile River by the Blue Nile. The lessening influence of the Blue Nile on Nile River streamflow during the fall season is a result of a declining Blue Nile and rising White Nile streamflow (Fig. 2). The Blue Nile to Sahel seasonal fractionation factors are greater than one except for the spring values. The temperature effect appears to weaken during this period with Nile River flow that may be influenced by regulation of streamflow from Aswan Dam (located in southern Egypt). Retention of water in Lake Nasser (reservoir behind Aswan Dam) would increase evaporation, but Lake Nasser provides a sufficient retention reservoir to mix the seasonal signals.

Table 3 Fractionation factors of median ratios of oxygen and hydrogen stable isotopes from precipitation and surface water samples collected in the Nile Basin

Season/site	Surface water (a) to precipitation (b)		Season/site	Surface water (a) to precipitation (b)	
	α of $^{18/16}O$	α of $^{2/1}H$		α of $^{18/16}O$	α of $^{2/1}H$
Fall			Winter		
Lake Victoria	1.0054	1.0314	Lake Victoria	1.0049	1.0255
White Nile	1.0008	1.0062	White Nile	1.0043	1.0265
Blue Nile	0.9988	0.9900	Blue Nile	0.9983	0.9832
Spring			Summer		
Lake Victoria	1.0063	1.0373	Lake Victoria	1.0044	1.0209
White Nile	1.0079	1.0468	White Nile	1.0029	1.0148
Blue Nile	1.0025	1.0088	Blue Nile	0.9998	0.9991

Note: Fractionation factor=$\alpha_{a-b}=R_a/R_b$; R=the ratio of the heavy isotope to the lighter isotope.

Table 4 Fractionation factors of median ratios of oxygen and hydrogen stable isotopes for comparing upstream to downstream locations in the Nile Basin

Sahel (a) to White Nile (b)			Sahel (a) to Blue Nile (b)			Mediterranean (a) to Sahel (b)		
Season	α of $^{18/16}O$	α of $^{2/1}H$	Season	α of $^{18/16}O$	α of $^{2/1}H$	Season	α of $^{18/16}O$	α of $^{2/1}H$
Fall	1.0017	1.0150	Fall	1.0021	1.0164	Fall	1.0027	NA
Winter	0.9995	0.9981	Winter	1.0043	1.0297	Winter	1.0011	1.0053
Spring	0.9974	0.9890	Spring	0.9996	0.9990	Spring	1.0001	0.9943
Summer	0.9980	0.9945	Summer	1.0014	1.0109	Summer	1.0034	1.0134

Note: Fractionation factor=$\alpha_{a-b}=R_a/R_b$; R=the ratio of the heavy isotope to the lighter isotope.

4 Conclusions

Seasonal isotopic signals (δ^2H and $\delta^{18}O$) are present for precipitation in the White Nile, Blue Nile and Nile River basins. Precipitation in the White Nile Basin is more similar to the Global Meteoric Water Line during winter and spring than precipitation in the Blue Nile Basin, but the opposite is true for summer and fall when the Blue Nile Basin receives moisture from the Indian Ocean monsoon. The inland moisture source in the White Nile Basin produces more depleted isotopic signals compared to precipitation in the Blue Nile Basin, but isotope values for precipitation in both of these basins typically are heavier than that for precipitation that falls in the northern Nile River Basin. A larger evaporation effect in the Sahel and Mediterranean (Sahara) regions of the Nile River Basin produces a precipitation isotopic signal with lower trendline slopes and smaller deuterium excess because of the transition from the predominantly tropical and subtropical climates of the White Nile and Blue Nile basins to the predominantly semi-arid and arid climates of the northern Nile River Basin. The hot temperatures of the Sahelian spring produce a greater evaporation signal in the precipitation isotope distribution compared to precipitation in the Sahara/Mediterranean region, which can be influenced by storms moving in from the Mediterranean Sea. The larger evaporative effect is reversed for these two regions in summer because of the cooling of the Sahel from inflow of Indian Ocean monsoon moisture that predominantly influences the Blue Nile Basin climate. The isotopic signals of the regional precipitation are visible in the streamflow of each region, which is further modified by additional evaporation according to the local climate. Isotope ratios for White Nile streamflow are significantly altered by evaporation in the Sudd, but this isotopic signal is minimized in the Nile River because of the flow dominance of the Blue Nile on the combined streamflow except during fall when the contribution from the White Nile may exceed that of the Blue Nile. The variation in climatic conditions of the Nile River Basin provides a means of identifying hydrologic mechanistic processes through changes in isotope ratios of hydrogen and oxygen, which have utility for separating precipitation origin and source waters during seasonal periods. The existing isotope record for precipitation and streamflow in the Nile River Basin can be used to evaluate predicted streamflow in the Nile River from a changing climate that is expected to induce further changes in precipitation patterns across the Nile River Basin.

Acknowledgements

The author acknowledges the assistance of the International Atomic Energy Agency's Water Resources Programme in compiling the isotope data collected from the Nile River Basin in the Isotope Hydrology Information System.

References

Abu-Zeid M A, El-Shibini F Z. 1997. Egypt's High Aswan Dam. International Journal of Water Resources Development, 13(2): 209–218.

Amarasekera K N, Lee R F, Williams ER, et al. 1997. ENSO and the natural variability in the flow of tropical rivers. Journal of Hydrology, 200: 24–39.

Awadallah A G, Rousselle J. 2000. Improving forecasts of Nile flood using SST inputs in TFN model. Journal of Hydrologic Engineering, 5(4): 371–379.

Beyene T, Lettenmaier D P, Kabat P. 2010. Hydrologic impacts of climate change on the Nile River Basin—implications of the 2007 IPCC climate scenarios. Climatic Change, 100 (3/4): 433–461.

Booij M J, Tollenaar D, van Beek E, et al. 2011. Simulating impacts of climate change on river discharges in the Nile Basin. Physics and Chemistry of the Earth, Parts A/B/C, 36(13): 696–709.

Buontempo C, Lørup J K, Antar M A, et al. 2009. Assessing the impacts of climate change on the water resources in the Nile Basin using a regional climate model ensemble. In: Climate Change and Water Systems: Global Risks, Challenges & Decisions. Copenhagen: Earth and Environmental Science IOP Conference Series, 6(29).

Camberlin P. 1997. Rainfall anomalies in the source region of the Nile and their connection with the Indian summer monsoon. Journal of Climate, 10(6): 1380–1392.

Conway D. 2005. From headwater tributaries to international river: observing and adapting to climate variability and change in the Nile Basin. Global Environmental Change, 15(2): 99–114.

Conway D, Hulme M. 1996. The impacts of climate variability and future climate change in the Nile Basin on water resources in Egypt. International Journal of Water Resources Development, 12(3): 277–296.

Conway D, Krol M, Alcamo J, et al. 1996. Future availability of water in Egypt: the interaction of global, regional, and basin scale driving forces in the Nile Basin. Ambio, 25(5): 336–342.

Craig H. 1961. Isotopic variations in meteoric waters. Science, 133: 1702–1703.

Craig H, Gordon L I. 1965. Deuterium and oxygen-18 variations in the ocean and the marine atmosphere. In: Lishi V, Pisa F. Proceedings of Stable Isotopes in Oceanographic Studies and Paleotemperatures. Spoleto, Italy: Geologic Nuclear Laboratory, 9–130.

Dansgaard W. 1964. Stable isotopes in precipitation. Tellus, 16: 436–468.

El-Asrag A M. 2005. Effect of synoptic and climatic situations on fractionation of stable isotopes in rainwater over Egypt and east Mediterranean. In: International Atomic Energy Agency, Isotopic Composition of Precipitation in the Mediterranean Basin in Relation to Air Circulation Patterns and Climate, IAEA-TECDOC-1453. Vienna, Austria, 51–73.

Eldaw A K, Salas J D, Garcia L A. 2003. Long-range forecasting of the Nile River flows using climatic forcing. Journal of Applied Meteorology, 42: 890–904.

Elshamy M E. 2009. Assessing the hydrological performance of the Nile Forecast System in long-term simulations. Nile Water Science & Engineering Journal, 1(3): 22–40.

Elshamy M E, Seierstad I A, Sorteberg A. 2009. Impacts of climate change on Blue Nile flows using bias-corrected GCM scenarios. Hydrology and Earth System Sciences, 13: 551–565.

Eltahir E A B. 1996. El Niño and the natural variability in the flow of the Nile River. Water Resources Research, 32(1): 131–137.

Gat J R, Carmi I. 1970. Evolution of the isotopic composition of atmospheric waters in the Mediterranean Sea area. Journal of Geophysical Research, 75(15): 3039–3048.

Gat J R, Dansgaard W. 1972. Stable isotope survey of the fresh water occurrences in Israel and the northern Jordan Rift Valley. Journal of Hydrology, 16(3): 177–211.

Gat J R. 2001. Atmospheric waters. In: Mook W G. Environmental Isotopes in the Hydrologic Cycle: Principles and Applications. Technical Documents in Hydrology, Vol. II. UNESCO, Paris, No. 39.

Gat J R, Klein B, Kushnir Y, et al. 2003. Isotope composition of air moisture over the Mediterranean Sea: an index of the air–sea interaction pattern. Tellus B, 55(5): 953–965.

Gleick P H. 1991. The vulnerability of runoff in the Nile Basin to climatic changes. The Environmental Professional, 13: 66–73.

Gonfiantini R, Fröhlich K, Araguas-Araguas L, et al. 1998. Chapter 7: isotopes in groundwater hydrology. In: Kendall C, McDonnell J J. Isotope Tracers in Catchment Hydrology. Amsterdam: Elsevier Science B.V., 203–246.

Guichard F, Kergoat L, Mougin E, et al. 2009. Surface thermodynamics and radiative budget in the Sahelian Gourma—seasonal and diurnal cycles. Journal of Hydrology, 375: 161–177.

Hoffmann G, Jouzel J, Masson V. 2000. Stable water isotopes in atmospheric general circulation models. Hydrological Processes, 14: 1385–1406.

Hulme M. 1994. Global climate change and the Nile Basin. In: Howell P P, Allan J A. The Nile: Sharing a Scarce Resource. Cambridge: Cambridge University Press, 139–162.

Hulme M, Doherty R, Ngara T, et al. 2001. African climate change: 1900–2100. Climate Research, 17(2): 145–168.

International Atomic Energy Agency (IAEA). 2005. Summary. In: International Atomic Energy Agency, Isotopic Composition of Precipitation in the Mediterranean Basin in Relation to Air Circulation Patterns and Climate. Vienna: International Atomic Energy Agency, IAEA-TECDOC-1453, 1–5.

International Atomic Energy Agency (IAEA). 2014. Global Network of Isotopes in Precipitation (GNIP). International Atomic Energy Agency, Water Resources Programme, Vienna. http://www-naweb.iaea.org/napc/ih/IHS_resources_gnip.html.

Johnson P A, Curtis P D. 1994. Water balance of Blue Nile River Basin in Ethiopia. Journal of Irrigation and Drainage Engineering, 120(3): 573–590.

Liotta M, Favara R, Valenza M. 2006. Isotopic composition of the precipitations in the central Mediterranean: origin marks and orographic precipitation effects. Journal of Geophysical Research: Atmospheres, 111(D19): 2156–2202.

Mathieu R, Pollard D, Cole J E, et al. 2002. Simulation of stable water isotope variations by the GENESIS GCM for modern conditions. Journal of Geophysical Research, 107(D4): 1–18.

Merlivat L, Jouzel J. 1979. Global climatic interpretation of the deuterium-oxygen 18 relationship for precipitation. Journal of Geophysical Research, 84(C8): 5029–5033.

Nicholson S E. 1994. Desertification. In: Schneider S H. Encyclopedia of Climate and Weather. New York: Oxford University Press, 239–242.

Noone D, Simmonds I. 2002. Associations between delta O-18 of water and climate parameters in a simulation of atmospheric circulation for 1979–95. Journal of Climate, 15: 3150–3169.

Poage M A, Chamberlain C P. 2001. Empirical relationships between elevation and the stable isotope composition of precipitation and surface waters: considerations for studies of paleoelevation change. American Journal of Science, 301: 1–15.

Quinn W H. 1992. A study of Southern Oscillation-related climatic activity for A.D. 622–1900 incorporating Nile River flood data. In: Diaz H F, Markgraf V. El Nino: Historical and Paleoclimatic Aspects of the Southern Oscillation. Cambridge, U.K.: Cambridge University Press, 119–149.

Risi C, Bony S, Vimeux F, et al. 2010. Understanding the Sahelian water budget through the isotopic composition of water vapor and precipitation. Journal of Geophysical Research, 115, D24110.

Rozanski K, Araguás-Araguás L, Gonfiantini R. 1993. Isotopic patterns in modern global precipitation. In: Swart P K, Lohmann K C, McKenzie J, et al. Climate Change in Continental Isotopic Records. Washington, D.C.: American Geophysical Union, Geophysical Monograph Series, 78: 1–36.

Sestini G. 1993. Implications of climate change for the Nile Delta. In: Sestini G. Climatic Change in the Mediterranean. London: Edward Arnold Publisher, 535–601.

Seleshi Y, Zanke U. 2004. Recent changes in rainfall and rainy days in Ethiopia. International Journal of Climatology, 24(8): 973–983.

Strzepek K, Yates D, Yohe G, et al. 2001. Constructing 'not implausible' climate and economic scenarios for Egypt. Integrated Assessment, 2(3): 139–157.

Sturm K, Hoffmann G, Langmann B, et al. 2005. Simulation of $\delta^{18}O$ in precipitation by the regional circulation model REMOiso. Hydrological Processes, 19: 3425–3444.

Sun L, Fredrick H M, Semazzi F G, et al. 1999. Application of the NCAR Regional Climate Model to eastern Africa: simulation of interannual variability of short rains. Journal of Geophysical Research: Atmospheres, 104(D6): 6549–6562.

Vörösmarty C J, Fekete B, Tucker B A. 1998. River discharge database, version 1.1 (RivDIS v1.0 supplement). Institute for the Study of Earth, Oceans, and Space/University of New Hampshire, Durham NH, USA.

Whetton P, Rutherfurd I. 1994. Historical ENSO teleconnections in the eastern hemisphere. Climatic Change, 28(3): 221–253.

Yates D N, Strzepek K M. 1998. Modeling the Nile Basin under climatic change. Journal of Hydrologic Engineering, 3(2): 98–108.

Appendix 1 Collection site information for isotope analysis of precipitation in the Nile Basin from the International Atomic Energy Agency's Global Network of Isotopes in Precipitation

Watershed	Collection site	Map (Fig. 1)	WMO no.	Altitude (m)	Climate	Sample	Collection period	Collector/Laboratory	Total $\delta^{18}O$	Total $\delta^{2}H$
White Nile	Equatorial Lake Plateau Region						1960–2009		479	462
	Kericho, Kenya	W1	6371401	2,130	3520-Cfb	Precipitation	1967–1971	University of Copenhagen (UC)	24	19
	Mugaga, Kenya	W2	6374101	2,070	3520-Cfb	Precipitation	1967–1968	UC	14	14
	Dar es Salaam, Tanzania	W3	6389400	55	1800- Aw	Precipitation	1960–1976	UC	125	118
	Dodoma, Tanzania	W4	6386200	1,120	2350-BSh	Precipitation	1993	Institute of Environmental Physics, University of Heidelberg	3	3
	Entebbe, Uganda	W5	6370500	1,155	1500-Af	Precipitation	1960–2006	UC	213	208
	Jinja, Uganda	W6	6370502	1,181	1500-Af	Precipitation	2003–2009	CNESTEN, Rabbat	27	27
	Kisoro, Uganda	W7	6372601	1,924	3520-Cfb	Precipitation	2001–2002	International Atomic Energy Agency (IAEA)	8	8
	Masaka, Uganda	W8	6370503	1,306	1800-Aw	Precipitation	2003–2009	CNESTEN, Rabbat	20	20
	Rukungiri, Uganda	W9	6372602	1,595	1800-Aw	Precipitation	2003–2006	PINSTECH, Islamabad	26	26
	Soroti, Uganda	W10	6365800	1,038	1800-Aw	Precipitation	1997–2009	IAEA	11	11
	Wobulenzi, Uganda	W11	6370504	1,150	1600-Am	Precipitation	1999–2000	Schonland Research Centre for Nuclear Sciences, University of the Witwatersrand, Johannesburg (SRCNS)	8	8
Blue Nile	Ethiopian Highlands (Ethiopia)						1961–2009		474	470
	Addis Ababa, Ethiopia	B1	6345000	2,360	3820-Cwb	Precipitation	1961–2009	UC	302	298
	Adu Bariye, Ethiopia	B2	6333001	1,832	2350-BSh	Precipitation	2002	Institute of Hydrologic GSF, Neuherberg (IHGFS)	5	5
	Alemeya, Ethiopia	B3	6347101	2,023	3820-Cwb	Precipitation	2002–2003	IAEA	13	13
	Asela, Ethiopia	B4	6346001	2,400	3820-Cwb	Precipitation	1994–1995	IAEA	7	7
	Awassa, Ethiopia	B5	6346000	1,750	1800-Aw	Precipitation	1995–2000	IHGFS	19	19
	Butajira, Ethiopia	B6	6345001	2,040	3820-Cwb	Precipitation	1995	IAEA	2	2
	Combolcha, Ethiopia	B7	6333300	1,929	3820-Cwb	Precipitation	2002	IHGFS	7	7
	Dessie, Ethiopia	B8	6333302	2,551	3820-Cwb	Precipitation	2002	IHGFS	8	8
	Diredawa, Ethiopia	B9	6347100	1,231	2350-BSh	Precipitation	2002–2003	IHGFS	12	12
	Hagere Selam, Ethiopia	B10	6346006	2,820	3520-Cfb	Precipitation	1999–2001	IHGFS	17	17
	Harar, Ethiopia	B11	6347102	1,924	3820-Cwb	Precipitation	2002	IAEA	6	6
	Hidolola, Ethiopia	B12	6361901	1,352	1800-Aw	Precipitation	1995	SRCNS	4	4
	Kobo, Ethiopia	B13	6333304	1,518	3810-Cwa	Precipitation	2002	IHGFS	7	7
	Kofele, Ethiopia	B14	6346002	2,680	3520-Cfb	Precipitation	1999–2000	IHGFS	15	15

Continued

Watershed	Collection site	Map (Fig. 1)	WMO no.	Altitude (m)	Climate	Sample	Collection period	Collector/Laboratory	Total $\delta^{18}O$	Total δ^2H
	Mega, Ethiopia	B15	6361902	1,254	1800-Aw	Precipitation	1995	SRCNS	4	4
	Moyale, Ethiopia	B16	6361900	1,090	1800-Aw	Precipitation	1995	SRCNS	4	4
	Neghelle, Ethiopia	B17	6353300	1,544	3820-Cwb	Precipitation	1995	SRCNS	3	3
	Silte, Ethiopia	B18	6345004	2,040	3820-Cwb	Precipitation	1995	IAEA	2	2
	Soddo, Ethiopia	B19	6346003	2,020	3520-Cfb	Precipitation	1999–2000	IHGFS	16	16
	Weldiya, Ethiopia	B20	6333303	1,920	3820-Cwb	Precipitation	2002	IHGSF	7	7
	Weledi, Ethiopia	B21	6333301	1,537	3810-Cwa	Precipitation	2002	IHGSF	8	8
	Yavello, Ethiopia	B22	6350001	1,778	3520-Cfb	Precipitation	1995	SRCNS	3	3
	Ziway, Ethiopia	B23	6346005	1,638	1800-Aw	Precipitation	1995	IAEA	3	3
Nile River, Sahel	Central Sudan						1962–1997		92	77
	Geneina, Sudan	S3	6277000	805	2350-BSh	Precipitation	1968–1976	UC	48	36
	Khartoum, Sudan	S6	6272100	382	2450-BWh	Precipitation	1960–1979	UC	44	41
Nile River, Sahara	Northern Egypt/Mediterranean						1961–2004		266	258
	Alexandria, Egypt	N1	6231800	7	2450-BWh	Precipitation	1961–2004	UC	87	78
	Cairo, Egypt	N2	6237100	34	2450-BWh	Precipitation	1968–2003	IAEA	19	19
	El-Arish, Egypt	N3	6233700	31	2450-BWh	Precipitation	1979–2003	IAEA	17	17
	Marsa Matruh, Egypt	N4	6230600	25	2450-BWh	Precipitation	1968–2003	IAEA	12	12
	Rafah, Egypt	N5	6233500	73	2450-BWh	Precipitation	2000–2003	IAEA	18	18
	Ras Eltine, Egypt	N6	6231700	15	2450-BWh	Precipitation	2001	IAEA	1	1
	Saint Catherene, Egypt	N7	6245700	1,350	2460-BWk	Precipitation	1979–2001	IAEA	2	2
	Siddi Barrani, Egypt	N8	6230100	24	2450-BWh	Precipitation	1978–2003	AGH University of Science and Technology, Krakow	110	111

Note: WMO, World Meteorological Organization; climate, WMO classification. The numbers in the last two columns indicate the number of samples for each isotope analysis.